



Original Paper

**Journal of Innovative Engineering
and Natural Science**

(Yenilikçi Mühendislik ve Doğa Bilimleri Dergisi)

<https://dergipark.org.tr/en/pub/jiens>

Properties of poly(2-ethyl aniline)/graphene oxide (PEAn/GO) nanocomposites: influence of a synthesis method and polymerization time

 Duygu Anaklı^a
^aSivas Cumhuriyet University, Faculty of Engineering, Department of Chemical Engineering, 58140 Sivas, Turkey

ARTICLE INFO

Article history:

Received 17 Nov 2024

Received in revised form 5 Jan 2025

Accepted 26 Jan 2025

Available online

Keywords:

Graphene oxide

Poly(2-ethyl aniline)

Nanocomposite

Polymerization

Electrical conductivity

ABSTRACT

In this work, the in situ polymerization of 2-ethyl aniline (2-EAn) in the presence of graphene oxide (GO) as an oxidant was carried out to synthesize conductive GO-poly(2-ethyl aniline) (PEAn) nanocomposites (GO-g-PEAn). GO-assisted GO-PEAn composite (GO-g-PEAn) refers to the chemical bonding and crystallisation of PEAn with a unique structure. The three different polymerization times, 48 h, 120 h and 240 h, were applied to analyze the effect of the reaction time on the polymerization of the composites. GO-PEAn nanocomposites were also synthesized by in situ polymerization of 2-EAn with the oxidant ammonium persulfate (APS), termed APS-GO-PEAn. GO-g-PEAn nanocomposites prepared at 120 h (5-day GO-g-PEAn) were selected as the most suitable composite based on evaluation of both scanning electron imaging and electrical conductivity characterization results. The 5-day GO-g-PEAn nanocomposites were compared with APS-GO-PEAn nanocomposites using X-ray diffraction (XRD) and scanning electron microscopy (SEM) analysis. The Fourier Transform Infrared (FTIR) spectrum confirmed the polymerisation of 2-ethyl aniline in the absence of conventional oxidants such as ammonium persulfate, potassium dichromate and potassium permanganate. XRD patterns indicate the presence of a crystalline phase of PEAn, resulting in higher conductivity in GO-g-PEAn nanocomposites than in APS-GO-PEAn nanocomposites. GO-g-PEAn nanocomposites showed promising conditions for their use as an electromagnetic interference (EMI) shielding materials.

I. INTRODUCTION

Due to their synergistic and superior physical and chemical properties (such as mechanical properties, electrical properties), graphene oxide/polyaniline (GO/PANI) composites have demonstrated applications in supercapacitors, sensors, adsorbents, solar cells, conductive dyes, electromagnetic interference (EMI) shielding materials and tissue engineering [1–8]. PANI is one of the most used conductive polymers to form composite materials and studied widely due to its promising features. For example, it exhibits better capacitance, flexibility, low cost, a wide range of electrical properties controlled by varying the doping levels and environmental stability [9, 12]. Although PANI has promising properties, it also has poor capabilities such as mechanical instability and early degradation [13]. The use of aniline derivatives to synthesize PANI polymers increases its potential to use in various application areas [12, 14]. For example, a derivative form of PANI, namely known as poly (2-ethyl aniline) (PEAn), enhanced poor solvent solubility and poor processability of PANI polymers as well as improved electrical conductivity with good chemical and oxidative stability [12, 15, 16].

A decision of suitable materials to make composite with PANI and their derivative forms mainly depends on desired properties for each application designed and new electronic properties expected based on morphological modifications or electronic interactions between the components [13, 17, 18]. Among the potential suitable materials (layered silicates, metal nanoparticles, ceramics) to form composites with PANI, graphene oxide (GO) has been widely employed as a graphene based starting material for the preparation of composites due to the

*Corresponding author. Tel.: +90-505-499-6765; e-mail: danakli@cumhuriyet.edu.tr

presence of many oxygen-containing functional groups [19]. In addition, its low production cost, improved mechanical stability, hydrophilic properties and ease of mass production have generated considerable interest in its potential applications in various scientific and industrial fields [20, 21]. The excellent properties of GO-assisted PANI composites have allowed them to exhibit improved characteristics, such as better energy density and performance, augmented strength, and superior durability. The obtained nanostructured composites also demonstrate excellent capacitance performance and good life cycles. Furthermore, the addition of GO has resulted in the improvement of the various electrical properties of the conductive PANI polymers [13].

There are several methods, including interfacial polymerization [22], electro-polymerization [19, 23] and in situ oxidative polymerization [24, 25] for various applications to produce PANI/GO composites. For example, in situ polymerization of aniline in the presence of GO sheets when ammonium persulfate (APS) used as a strong oxidant has been performed for preparation of GO-PANI nanocomposites due to its ease-going synthesis procedure and rapid oxidative reaction. Each PANI based nanocomposite preparation technique results in composites with different properties such as electrical conductivity, depending on the type of bonding structures formed between GO and PANI [26]. Zhao et al. [27] observed that the in situ polymerization of aniline by using GO nanosheets introduced a charge transfer from the interaction between the aniline and the graphene oxide, and also improved the electrical conductivity in the GO-PANI composite forms compared to pristine PANI. However, it is still a challenge to prepare the composites in a preferred state and specifications at low cost. Mutalib et al. 2021 prepared PANI/GO nanocomposites by a solution method with different weight percent of GO. The electrical conductivity of composites decreased with increasing GO loading and the highest electrical conductivity reached up to $1.83 \times 10^{-10} \text{ S cm}^{-1}$ with the 50 wt % GO loading [8]. Moghadam et al., 2014 prepared GO-PANI nanocomposites by in situ polymerization of aniline in the presence of GO as oxidant. The synthesized GO-PANI composites obtained by using GO oxidant exhibited higher electrical conductivity of 5.83 S cm^{-1} compared to 0.203 S cm^{-1} for GO-PANI obtained by APS assisted polymerization [26].

In the present work, 2-ethyl aniline was used instead of aniline, which was used in the study by Moghadam et al. (2014). The other difference is the polymerization time, 120 h was found to be sufficient for polymerization, which was less than the 240 h used. The use of GO as an oxidant for the synthesis of GO-g-PEAn nanocomposites by in situ polymerization of 2-ethyl aniline has not been studied so far. Thus, the present research work investigates the production of GO assisted GO-PEAn (GO-g-PEAn) nanocomposites by changing the duration of polymerization during a GO-g-PEAn nanocomposite synthesis process to discern alterations in their properties. In addition, GO-PEAn nanocomposites were also synthesized using a conventional oxidant APS via in situ polymerization for a comparison view. Structural and surface morphology, and electrical properties of the nanocomposite samples achieved are examined by Fourier transform infrared spectroscopy (FTIR), X-ray diffraction analysis (XRD), and scanning electron microscopy (SEM) and are evaluated. Moreover, the electrical conductivity behaviour of the resultant nanocomposites was analyzed and assessed.

II. EXPERIMENTAL METHOD

2.1 Materials

Graphite flakes (+100 mesh ($\geq 75\%$ min)) and sulphuric acid (H_2SO_4) (95-97%) were supplied from Sigma-Aldrich (Saint Louis, MO, USA). Phosphoric acid (H_3PO_4) (65%), potassium permanganate (KMnO_4), hydrochloric acid

(HCl) (37% fuming), and hydrogen peroxide (H_2O_2) were purchased from Merck. These starting materials were used to prepare graphene oxide nanosheets. For poly(2-ethyl aniline) (PEAn) polymer synthesis and subsequently, its preparation as a nanocomposite material, 2-ethyl aniline (2-EAn, Merck) monomer, an oxidant material, ammonium persulfate (APS, $(NH_4)_2S_2O_8$, 98 wt %) and nitric acid (HNO_3) (65%) liquid were provided by Sigma-Aldrich. All the experiments in this research work were performed using deionized (DI) water (18 M Ω). All chemicals were used as received without any treatment or further purification.

2.2 Preparation Techniques

2.2.1. Preparation of graphene oxide (GO) nanosheets

Graphene oxide (GO) nanosheets were synthesized from commercially received graphite flakes in aqueous solution using the Modified Hummers' method [28]. 30% hydrogen peroxide was added to the mixture to reduce residual permanganate. The graphite oxide was thoroughly washed several times with pure DI water to remove residual strong organic acids and other reagents such as sulfate and phosphate ions. This process continued until pH=7.0 and then dried under vacuum at 60 °C overnight. The graphite oxide was dried, resuspended in DI water, and exfoliated into GO nanosheets.

In order to confirm successful synthesis of graphene oxide nanosheets, FTIR, XRD and SEM investigations were carried out.

2.2.2. Preparation of poly(2-ethyl aniline) PEAn polymer

Pure PEAn polymer was synthesized by an oxidative chemical polymerization of 2-EAn monomer by following the polymerization route addressed in [29]. FTIR analysis was carried out to confirm the synthesis of poly (2-ethyl aniline) polymer.

2.2.3. In situ synthesis of APS-GO-PEAn nanocomposites and GO-g-PEAn nanocomposites

Ammonium persulfate-assisted GO enriched PANI polymerization (APS-GO-PANI) has been described previously [26]. In the present study, APS assisted GO enriched PANI derivative "PEAn" based nanocomposites were prepared first time within an in situ polymerization of 2-EAn and the traditional oxidant ammonium persulfate (APS). 1.37 mL of 2-EAn was dissolved in 1 M HCl and mixed in a magnetic stirrer for 30 min. This mixture was then added to an aqueous GO solution (1 mg ml⁻¹) prepared in an ultrasonic bath. Approximately 0.625 g of APS was dissolved in 10 mL of 1 M HCl. It was then added drop by drop to the reaction vessel containing 2-EAn and GO. After two hours of polymerization, the product was filtered and washed three times with DI water and 1 M HCl to give APS-GO-PEAn.

On the other hand, synthesis of GO-g-PEAn nanocomposites was carried out according to the method applied by Moghadam et al. [26]. 1.37 ml of 2-EAn and 1 mg ml⁻¹ of aqueous GO solution were used as for the GO-g-PEAn synthesis. The procedure was performed by changing polymerization duration as of 48 h, 120 h and 240 h in the the reaction environment where samples left at room temperature. The resulting mixtures were centrifuged and washed with DI water and 1 M HCl. The products were kept at room temperature overnight to prepare the GO-g-

PEAn nanocomposite. In order to determine the effect of the reaction time on the polymerization of the nanocomposites as well as their features, polymerization duration was adjusted. A schematic representation of the synthesis procedure of the achieved nanocomposites is shown in Figure 1. The structure, crystallinity and morphological properties of these composites formed were characterized by couple of analytical techniques, including FTIR, XRD analysis and SEM imaging investigation.

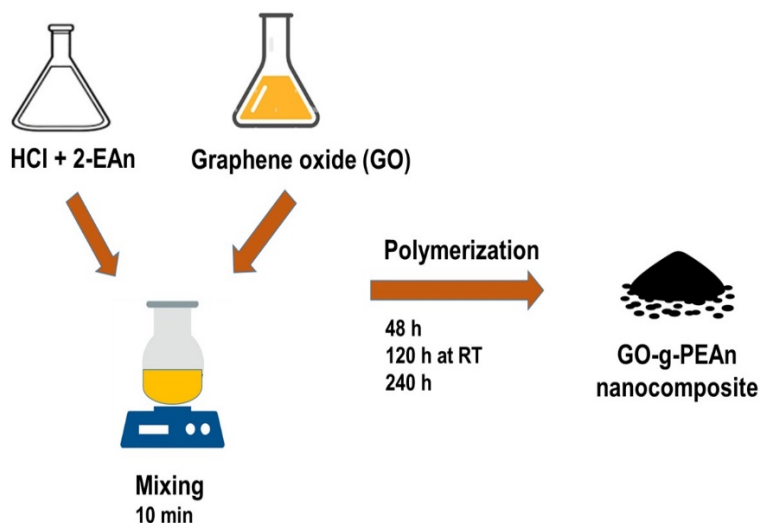


Figure 1. Schematic representation of the fabrication process of Graphene-g-PEAn nanocomposites (Color figure online)

2.3 Physicochemical Characterizations

ATR-FTIR measurements were performed on the starting materials, GO-g-PEAn and APS-GO-PEAn composites prepared using a Bruker Alpha 1003271/06 IR spectrometer (Bruker, Karlsruhe, Germany). Spectrums were recorded with a resolution of 1 cm^{-1} and 20 scans per spectrum in the wavenumber range from 400 cm^{-1} to 4000 cm^{-1} . Peaks were assigned and compared to specific chemical bonds based on previously examined studies of similar materials. The XRD spectrum of GO and the composites was obtained using a Rigaku Miniflex 600 X-ray diffractometer (Rigaku, Tokyo, Japan) to describe the structural characterization of the samples, including the phase composition, crystallinity of the materials and identification of interlayer changes in the materials. The analysis was performed using $\text{CuK}\alpha$ radiation ($\lambda = 1.5405\text{ \AA}$) at a voltage of 40 kV and a current of 15 mA. Samples were scanned from 2° to 80° at a scan rate of 5 min^{-1} . Morphological features were conducted using a field emission scanning microscope (FE-SEM, Tescan Mira3 XMU, Czech Republic). Prior to SEM analysis, the samples were coated with a thin gold layer to make them conductive for getting better resolution.

2.4 Electrical Conductivity Performance Tests of Samples

The electrical conductivity features of the samples produced were described using a digital multimeter (UNIT, UT70B), the two-probe method at room temperature environment. The two electrodes of the multimeter device system were placed over the sample to measure the resistance of the resultant samples by adjusting ten different points and performing these measurements seven times per sample. Subsequently, the electrical conductivity was

calculated by using data collected [30]. Initially, the specimens for electrical conductivity measurement were prepared with making them pellet form. To form the nanocomposite pellets, nanocomposite powders were compressed into a pellet form with a diameter of 1.13 cm and a thickness of 1.0 mm by using an 8-ton hydraulic press.

III. RESULTS AND DISCUSSIONS

3.1. Characterization of Graphene Oxide

Graphene oxide nanosheets were successfully synthesized using the Modified Hummers' method. The brown colour obtained is evidence of the oxygen functional groups in the GO nanosheets and is shown in Figure 2a. The surface morphology of the GO nanosheets was examined by field emission scanning electron microscopy (FESEM) to confirm the sheet-like structure, while X-ray diffraction (XRD) was used to verify the purity, structural information and formation of the GO nanosheets. A typical FESEM image of the prepared GO is shown in Figure 2b, which shows GO nanosheets with wrinkled surfaces [31].

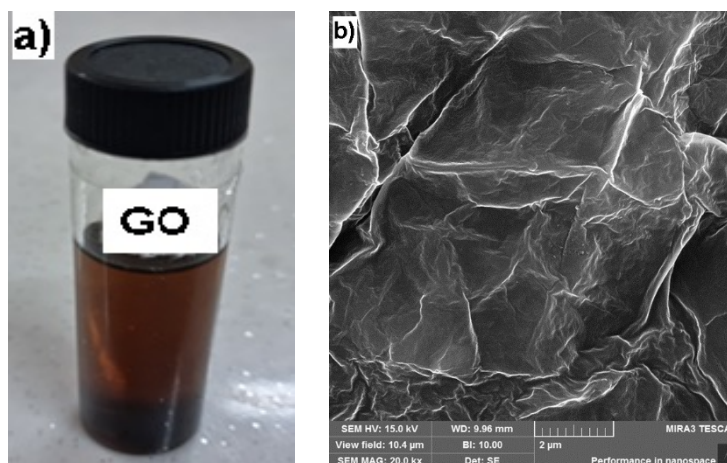


Figure 2. (a) Digital picture of GO nanosheets and (b) FESEM image of GO nanosheets achieved from the Modified Hummers' method in this work

The XRD measurement (Figure 3) showed a typical peak at 10.19° corresponding to the (002) basal plane with a d-spacing of 8.6730 \AA and an FWHM of 0.721 degrees. The high d-spacing indicates the successful of exfoliation of graphite sheets and this main peak proves the formation of sheets with oxygen containing functional groups, such as epoxy, hydroxy, carbonyl and carboxyl groups. The prepared GO also gives peaks at $2\theta = 20.25^\circ$ and 42.48° . The absence of peaks at about 26° proves the conversion of all graphite sheets into graphene oxide nanosheets [32, 33]. Based on the above-mentioned results, the GO nanosheets synthesized were used to produce GO enriched nanocomposite structures in this research work.

GO-g-PEAn nanocomposites were successfully prepared by in situ polymerization of 2-EAn using GO as an oxidant. In the literature, GO-g-PANI nanocomposites have been prepared for 240 h under room temperature conditions. In order to determine whether a shorter polymerization time would be sufficient for polymerization,

the reaction vessels were left at room temperature for 48 h, 120 h and 240 h. The optimum polymerization time was determined from the SEM images and electrical conductivity data. The results of the analyses demonstrated that the GO-g-PEAn nanocomposites prepared at 120 h (5-day GO-g-PEAn) were selected as the most suitable nanocomposites.

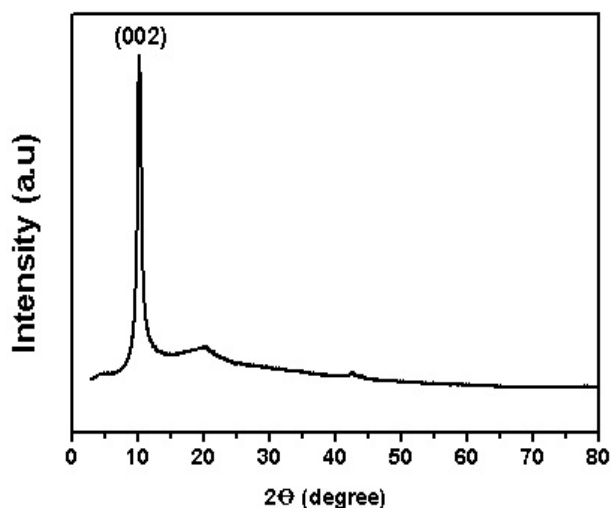


Figure 3. XRD pattern of GO nanosheets achieved from the Modified Hummers' method in this work

3.2. Estimation of Polymerization Time Effect on GO-g-PEAn Nanocomposite Preparation

The dashed area in the SEM images shows only the graphene oxide layers (Figure 4a). For the 2-day GO-g-PEAn nanocomposites, a small amount of polymer was seen on the surfaces of the graphene oxide layers, indicating insufficient polymerization, resulting in the lowest electrical conductivity compared to other nanocomposites. Figure 4b shows that the GO layers appeared smooth and undamaged. 2-EAn monomer was polymerized on the GO layers and integrated between these layers to form a sandwich structure. Figure 4c shows the PEAn polymer bridging on the surface of the graphene oxide layers. This PEAn polymer bridges between the GO sheets, resulting in an interconnected network with higher electrical conductivity.

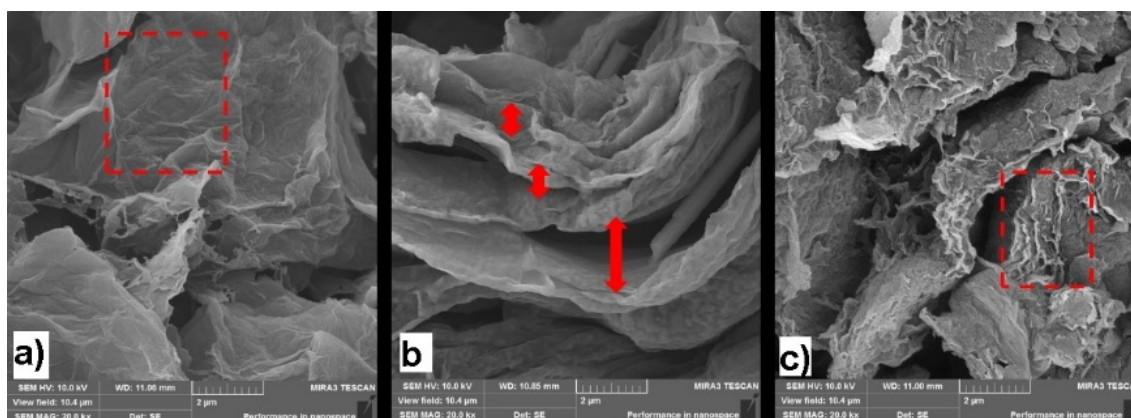


Figure 4. SEM images, (a) 2-day GO-g-PEAn, (b) 5-day GO-g-PEAn and (c) 10-day GO-g-PEAn

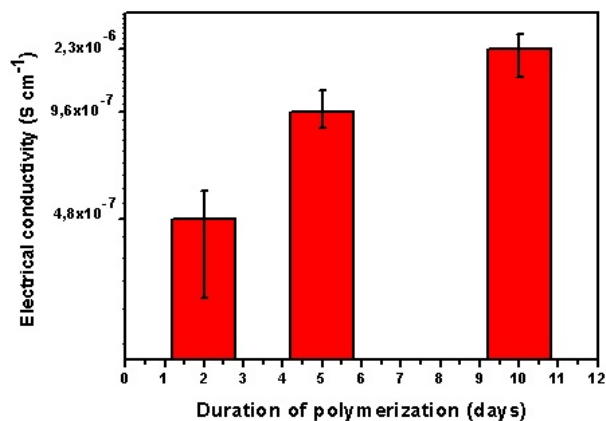


Figure 5. Electrical conductivity of the prepared GO-g-PEAn nanocomposites at different duration of polymerizations applied

As shown in Figure 5, it was observed that the composites with the highest conductivity among the GO-g-PEAn nanocomposites prepared at different polymerisation times were the 10 days GO-g-PEAn nanocomposites ($2.33 \times 10^{-6} \text{ Scm}^{-1}$). Since the electrical conductivity values obtained from the 2-day GO-g-PEAn nanocomposite were quite low ($4.83 \times 10^{-7} \text{ Scm}^{-1}$) and close to the pure PEAn value ($3.5 \times 10^{-7} \text{ Scm}^{-1}$), it was suggested that the 2-day polymerization time was insufficient for the composite preparation. After 10 days polymerization time applied which is quite long and 2 days polymerization duration appears insufficient for composite preparation, and the electrical conductivity value of 5 days GO-g-PEAn nanocomposites ($9.62 \times 10^{-7} \text{ Scm}^{-1}$) is nearby to 10 days GO-g-PEAn nanocomposites, 5 days polymerisation time was considered sufficient for GO-g-PEAn nanocomposite preparation.

From both the SEM images captured and the electrical conductivity performance results collected, the best GO-g-PEAn nanocomposite with enhanced features could be prepared by 5 days polymerization processed specimens. These nanocomposite specimens were then compared with the APS-GO-PEAn nanocomposites by using data collected by FTIR, XRD, and SEM investigations.

3.3. Comparison of GO-g-PEAn with APS-GO-PEAn Nanocomposites Prepared

The ATR-FTIR spectra of PEAn, GO, GO-g-PEAn, and APS-GO-PEAn are shown in Figure 6, together with the chemical structure of the samples. In Figure 6a, the characteristic peaks of PEAn polymer appeared at 1587 cm^{-1} and 1496 cm^{-1} correspond to the C=N and C-N stretching of the quinoid and benzenoid rings of PEAn, respectively. The peak at 1261 cm^{-1} is attributed to the polaron structure of PEAn resulting from the C-N⁺ stretching vibration. The band at 813 cm^{-1} is associated with the out-of-plane deformation of C-H in the 1,4-disubstituted benzene ring. The C-H bending vibrations appeared at 2930 cm^{-1} and the peak at 1120 cm^{-1} is attributed to the in-plane aromatic C-H bending vibrations. The successful synthesis of the PEAn polymer was confirmed with evidence received by an ATR-FTIR spectral measurement. The results were similar to those reported in the literature [34-37]. For GO nanosheets, the broad peak observed between the wavelengths of 3000 and 3500 cm^{-1} is assigned to the -OH stretching vibrational mode, indicating the presence of hydroxyl groups in the structure (Figure 6b). One of the characteristic peaks of GO nanosheets is observed at 1726 cm^{-1} due to the C=O stretching vibrations of the carbonyl

and carboxylic groups. The unoxidized graphitic region (C=C stretching) is observed at 1620 cm^{-1} . The epoxy or alkoxy C–O stretching peak is also present at 1040 cm^{-1} [26, 31, 38, 39].

Polymerization of 2-EAn was indicated by the appearance of characteristic peaks of both PEAn and GO nanosheets in the spectrum of GO-g-PEAn and APS-GO-PEAn nanocomposites. The absence of the peak of GO nanosheets at 1620 cm^{-1} in the nanocomposites indicates the reduction of unstable graphitic double bonds during polymerization. However, the peak intensities in the nanocomposites have decreased compared to PEAn, indicating an increased stability of the prepared nanocomposites [40]. On the other hand, a significant increase in peak intensities was observed in the FTIR spectrum of the GO-g-PEAn nanocomposite compared to that of the APS-GO-PEAn nanocomposites. This indicated that the delocalisation of electrons resulted in an enhancement in the electrical conductivity of the GO-g-PEAn nanocomposites, as evidenced by previous studies [16, 18].

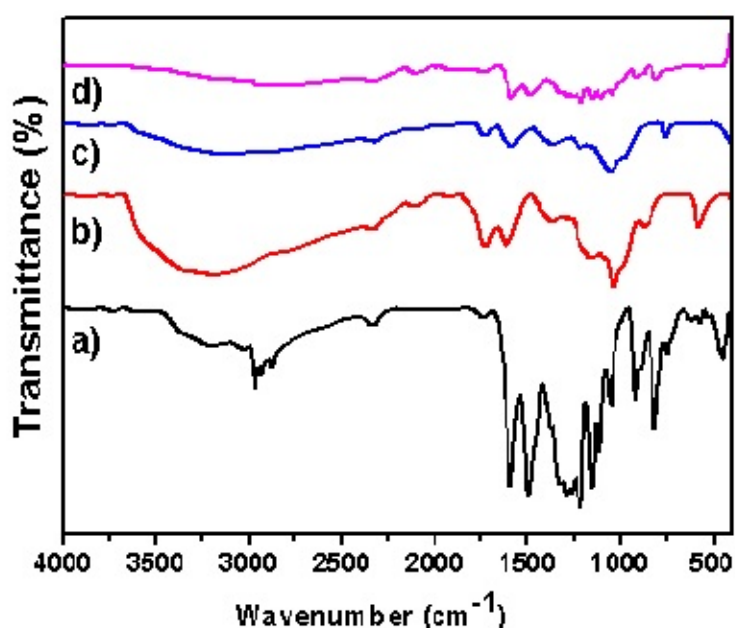


Figure 6. FTIR spectra of PEAn (a), GO (b), GO-g-PEAn (c), and APS-GO-PEAn (d)

The crystallinity of the GO-g-PEAn and APS-GO-PEAn nanocomposites achieved was determined from the XRD patterns obtained. The GO-g-PEAn nanocomposites (Figure 7a) show sharper peaks than the APS-GO-PEAn nanocomposites produced at 10.09° and 42.45° . In the XRD pattern of GO-g-PEAn there is a small amorphous phase related to PEAn, and with the other peaks indicating the presence of PEAn and GO in the structure. The diffraction peaks at 10.09° , 20.79° , 27.42° , 31.71° corresponds to (001), (100), (111) and (020) planes, respectively. The diffraction peaks for PEAn appeared at $2\theta = 14.05^\circ$ and 24.3° , corresponding to the (011) and (200) planes of the polymer in its emeraldine salt, respectively. In the XRD pattern of APS-GO-PEAn (Figure 7b), there is a more pronounced amorphous phase associated with PEAn than in the GO-g-PEAn structure. This difference is due to the newly ordered structure of PEAn in GO-g-PEAn compared to APS-GO-PEAn. The structure in GO-g-PEAn probably shows that polymer chain growth would form on the GO sheets, leading to crystallization [26].

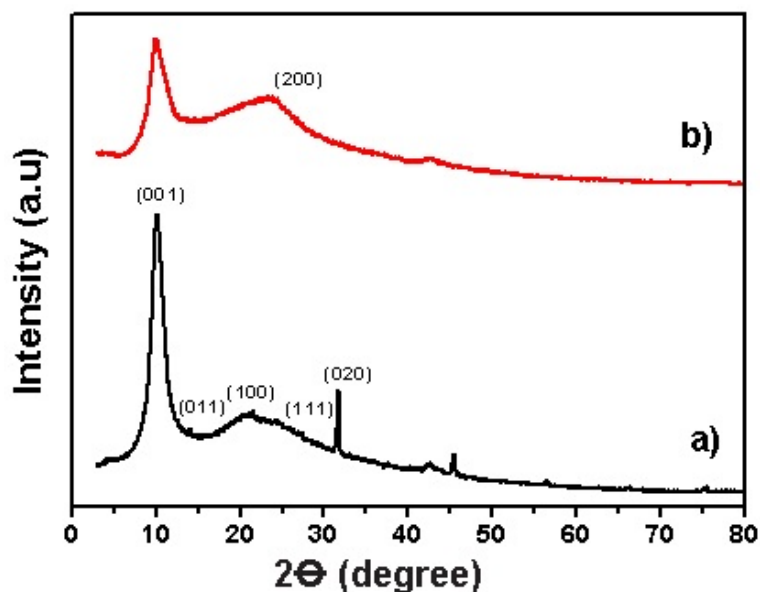


Figure 7. XRD patterns of GO-g-PEAn nanocomposite (a) and APS-GO-PEAn nanocomposite (b)

The SEM image (Figure 8a) shows that the PEAn particles are aligned on the surfaces of the GO nanosheets and intercalated between the GO layers. This composite structure was obtained with wide and layered GO sheets and granular PEAn polymer, inducing a crystalline structure with high electrical conductivity. The arrows in Figure 8a indicate the wide and smooth GO sheets. For the APS-GO-PEAn nanocomposite, the GO nanosheets were unevenly distributed uniformly within the PEAn matrix. The PEAn particles aligned in a disordered manner on the surfaces of the GO sheets, and agglomerations and aggregates of PEAn polymer were seen, resulting in low conductivity compared to GO-g-PEAn nanocomposites. The dashed area indicates the agglomerations of PEAn polymer and the arrows represent the GO sheets (Figure 8b).

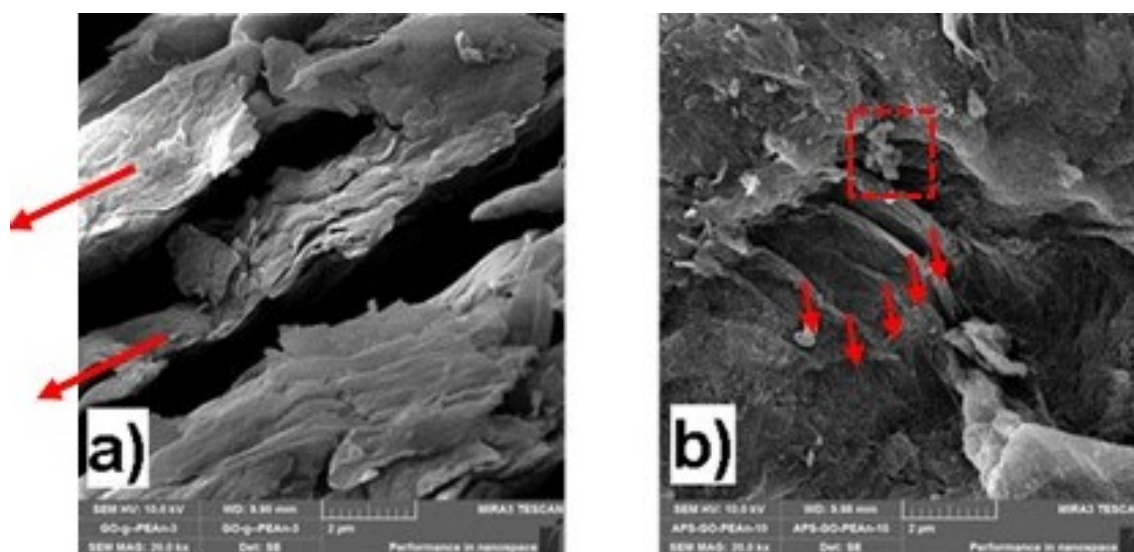


Figure 8. SEM images, (a) GO-g-PEAn nanocomposites and (b) APS-GO-PEAn nanocomposites

The schematic has been drawn to explain the composite structure in composites as shown in Figure 9. Both composites show intercalated structure and PEAn polymer aligned on graphene oxide layers.

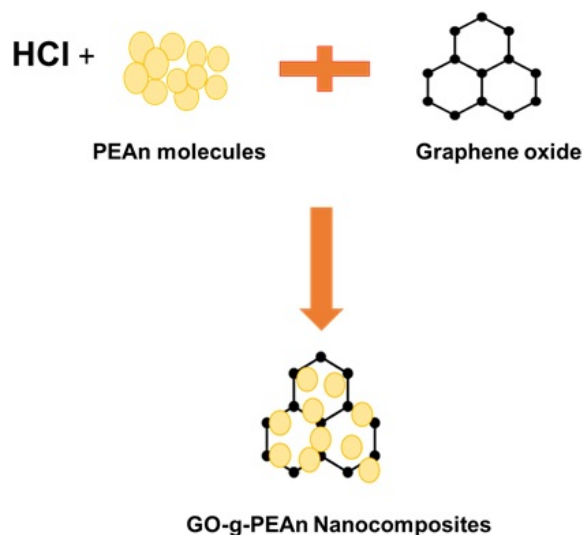


Figure 9. The schematics showing the composite structure in GO-g-PEAn nanocomposites.

The electrical conductivity of pure PEAn, GO-g-PEAn and APS-GO-PEAn composites were determined by measuring the resistivity of the samples using the two-probe method. Due to the insulating nature of GO with a low conductivity of $4.57 \times 10^{-8} \text{ S cm}^{-1}$, the addition of PEAn, which has an electrical conductivity of $3.5 \times 10^{-7} \text{ S cm}^{-1}$, to the GO structure resulted in an improvement in the conductivity of the resulting composite [41, 42]. However, the electrical conductivity of the APS-GO-PEAn nanocomposite is $5.03 \times 10^{-7} \text{ S cm}^{-1}$, which is significantly lower than that of the 5-day GO-g-PEAn nanocomposites of $9.62 \times 10^{-7} \text{ S cm}^{-1}$. This finding indicates that the electrical conductivity of the 5-day GO-g-PEAn nanocomposite has increased by approximately 0.5 order compared to the APS-GO-PEAn nanocomposite. Mutalib et al. 2021 [8], prepared GO/PANI composites with high GO (50 wt%) and showed an electrical conductivity of $1.83 \times 10^{-10} \text{ S cm}^{-1}$. This value was lower than that of the electrical conductivity of the nanocomposites prepared in this study, despite the use of PEAn polymer, which has a lower conductivity than PANI.

IV. CONCLUSIONS

As a new approach, highly conductive GO-PEAn nanocomposite materials (GO-g-PEAn) supported by GO nanosheets were successfully obtained. In this synthesis method, the nanocomposite material was obtained by in situ polymerization of 2-ethyl aniline in the presence of GO nanosheets as an oxidant. The favourable polymerization conditions also induced high crystallinity, alignment and chemical bonding between the PEAn and GO nanosheet structures. In the FTIR spectrum of GO-g-PEAn nanocomposites, a significant increase in peak intensities was observed compared to that of APS-GO-PEAn nanocomposites. The increase in electrical conductivity of GO-g-PEAn nanocomposites appears to be due to electron delocalisation. The electrical conductivity value of the GO-g-PEAn nanocomposites obtained within 5 days of polymerization time ($9.62 \times 10^{-7} \text{ S cm}^{-1}$) is significantly higher than the electrical conductivity value of both components and the prepared APS-GO-PEAn nanocomposites ($5.03 \times 10^{-7} \text{ S cm}^{-1}$) which could be caused by the delocalization of electrons. The GO-g-PEAn nanocomposites show high electrical conductivity, which supports the FTIR results, because of the higher

crystallinity and/or chemical grafting of the PEAn polymer onto the GO nanosheets. It has been demonstrated that GO-g-PEAn nanocomposites have the capacity to be utilised as EMI shielding materials.

ACKNOWLEDGMENT

This study was financially supported by Sivas Cumhuriyet University Scientific Research Project (CUBAP), project number M-2021-820.

REFERENCES

1. Yan X, Chen J, Yang J, Xue Q, Miele P (2010) Fabrication of free-standing, electrochemically active, and biocompatible graphene oxide-polyaniline and graphene-polyaniline hybrid papers. *ACS Appl Mater Interfaces* 2:2521–2529. <https://doi.org/10.1021/am100293r>
2. Wang H, Hao Q, Yang X, Lu L, Wang X (2009) Graphene oxide doped polyaniline for supercapacitors. *Electrochem. Commun* 11:1158–1161. <https://doi.org/10.1016/j.elecom.2009.03.036>
3. Yu H, Wang T, Wen Bo, Lu M, Xu Z, Zhu C, Chen Y, Xue X, Sun C, Cao M (2012) Graphene/polyaniline nanorod arrays: synthesis and excellent electromagnetic absorption properties. *J Mater Chem* 22:21679–21685. <https://doi.org/10.1039/C2JM34273A>
4. Hsu YC, Chen G L, Lee RH (2014) Graphene oxide sheet-polyaniline nanocomposite prepared through in-situ polymerization/deposition method for counter electrode of dye-sensitized solar cell. *J Polym Res* 21, 440. <https://doi.org/10.1007/s10965-014-0440-5>
5. Hong X, Fu J, Liu Y, Li S, Wang X, Dong W, Yang S (2019) Recent progress on graphene/polyaniline composites for high-performance supercapacitors. *Materials* 12, 1451. <https://doi.org/10.3390/ma12091451>
6. Shakir MF, Khan AN, Khan R, Javed S, Tariq A, Azeem M, Riaz A, Shafqat A, Cheema HM, Akram MA, Ahmad I, Jan R (2019) EMI shielding properties of polymer blends with inclusion of graphene nano platelets. *Results Phys* 14, 102365. <https://doi.org/10.1016/j.rinp.2019.102365>
7. Cai X, Lai L, Shen Z, Lin J (2017) Graphene and graphene-based composites as Li-ion battery electrode materials and their application in full cells. *J Mater Chem A* 5:15423–15446. <https://doi.org/10.1039/C7TA04354F>
8. Mutalib TNABTA, Tan SJ, Foo KL, Liew YM, Heah CY, Abdullah MMAB (2021) Properties of polyaniline/graphene oxide (PANI/GO) composites: effect of GO loading. *Polymer Bulletin* 78: 4835–4847. <https://doi.org/10.1007/s00289-020-03334-w>
9. Dhawan SK, Kumar D, Ram MK, Chandra S, Trivedi DC (1997) Application of conducting polyaniline as sensor material for ammonia. *Sens Actuators B* 40:99-103. [https://doi.org/10.1016/S0925-4005\(97\)80247-X](https://doi.org/10.1016/S0925-4005(97)80247-X)
10. Song E, Choi JW (2013) Conducting polyaniline nanowire and its applications in chemiresistive sensing. *Nanomaterials* 3:498–523. <https://doi.org/10.3390/nano3030498>
11. Goswami S, Maiti UN, Maiti S, Nandy S, Mitra MK, Chattopadhyay KK (2011) Preparation of graphene–polyaniline composites by simple chemical procedure and its improved field emission properties. *Carbon* 49:2245–2252. <https://doi.org/10.1016/j.carbon.2011.01.055>
12. Sebastian J, Samuel JM (2020) Recent advances in the applications of substituted polyanilines and their blends and composites. *Polym Bull* 77:6641–6669. <https://doi.org/10.1007/s00289-019-03081-7>
13. Balboa-Palomino A, Páramo-García U, Melo-Banda JA, Verde-Gómez JY, Gallardo-Rivas NV (2024) Effect of Graphene Oxide addition on the properties of electrochemically synthesized polyaniline–graphene oxide films. *Polymers* 16(12):1677. <https://doi.org/10.3390/polym16121677>
14. Bissessur R, White W (2006) Novel alkyl substituted polyanilines/molybdenum disulfide nanocomposites. *Mater Chem Phys* 99:214–219. <https://doi.org/10.1016/j.matchemphys.2005.10.012>
15. Thanokiang J, Sakunpongpitorn P, Direksilp C, Choichom P, Phasuksom K, Paradee N, Sirivat A (2019) Synthesis and characterization of conducting poly(2-ethylaniline) nanoparticle: Effect of surfactant template on morphology and electrical conductivity. *Synth Met* 256. <https://doi.org/10.1016/j.synthmet.2019.116142>
16. Luo J, Jiang S, Wu Y, Chen M, Liu XJ (2012) Synthesis of stable aqueous dispersion of graphene/polyaniline composite mediated by polystyrene sulfonic acid. *Polym Sci Part A: Polym Chem* 50:4888–4894. <https://doi.org/10.1002/pola.26316>

17. Gao Z, Wang F, Chang J, Wu D, Wang X, Wang X, Xu F, Gao S, Jiang K (2014) Chemically grafted graphene-polyaniline composite for application in supercapacitor. *Electrochim Acta* 133:325–334. <https://doi.org/10.1016/j.electacta.2014.04.033>
18. Elnaggar EM, Kabel KI, Farag AA, Al-Gamal AG (2017) Comparative study on doping of polyaniline with graphene and multi-walled carbon nanotubes. *J Nanostructure Chem* 7:75–83. <https://doi.org/10.1007/s40097-017-0217-6>
19. Wei H, Zhu J, Wu S, Wei S, Guo Z (2013) Electrochromic polyaniline/graphite oxide nanocomposites with endured electrochemical energy storage. *Polymer* 54:1820–1831. <https://doi.org/10.1016/j.polymer.2013.01.051>
20. Li J, Zeng X, Ren T, Van der Heide E (2014) The preparation of graphene oxide and its derivatives and their application in bio-tribological systems. *Lubricants* 2:137–161. <https://doi.org/10.3390/lubricants2030137>
21. Raji M, Zari N, Abou el Kacem Qaiss RB (2019) Chemical preparation and functionalization techniques of graphene and graphene Oxide, in functionalized graphene nanocomposites and their derivatives, Elsevier, Amsterdam, ss 1–20.
22. Nguyen VH, Tang L, Shim J-J (2013) Electrochemical property of graphene oxide/polyaniline composite prepared by in situ interfacial polymerization. *Colloid Polym Sci* 291:2237–2243. <https://doi.org/10.1007/s00396-013-2940-y>
23. Jiang X, Lou S, Chen D et al (2015) Fabrication of polyaniline/graphene oxide composite for graphite felt electrode modification and its performance in the bioelectrochemical system. *J Electroanal Chem* 744:95–100. <https://doi.org/10.1016/j.jelechem.2015.03.001>
24. Moon Y-E, Yun J, Kim H-I (2013) Synergetic improvement in electromagnetic interference shielding characteristics of polyaniline-coated graphite oxide/ γ -Fe₂O₃/BaTiO₃ nanocomposites. *J Ind Eng Chem* 19:493–497. <https://doi.org/10.1016/j.jiec.2012.09.002>
25. Zheng J, Ma X, He X et al (2012) Preparation, characterizations, and its potential applications of PANI/graphene oxide nanocomposite. *Procedia Eng* 27:1478–1487. <https://doi.org/10.1016/j.proeng.2011.12.611>
26. Mohamadzadeh Moghadam MH, Sabury S, Gudarzi MM, Sharif F (2014) Graphene oxide-induced polymerization and crystallization to produce highly conductive polyaniline/graphene oxide composite. *J Polym Sci Part A Polym Chem* 52:1545–1554. <https://doi.org/10.1002/pola.27147>
27. Zhao Y, Tang G-S, Yu Z-Z, Qi J-S (2012) The effect of graphite oxide on the thermoelectric properties of polyaniline. *Carbon* 50:3064–3073. <https://doi.org/10.1016/j.carbon.2012.03.001>
28. Hummers WS, Offeman RE (1958) Preparation of Graphitic Oxide. *J Am Chem Soc* 80(6), 1339. <https://doi.org/10.1021/ja01539a017>
29. Zhao X, Gnanaseelan M, Jehnichen D, Simon F, Pionteck J (2019) Green and facile synthesis of polyaniline/tannic acid/rGO composites for supercapacitor purpose. *J Mater Sci* 54:10809–10824. <https://doi.org/10.1007/s10853-019-03654-x>
30. Jun YS, Um JG, Jiang G, Yu A (2018) A Study on the effects of graphene nano-platelets (GnPs) sheet sizes from a few to hundred microns on the thermal, mechanical, and electrical properties of polypropylene (PP)/GnPs composites. *Express Polym Lett* 12:885–897. <https://doi.org/10.3144/expresspolymlett.2018.76>
31. Anaklı D, Erşan M (2024) Optimization of reduced graphene oxide yield using response surface methodology. *Diamond Relat Mater* 148. <https://doi.org/10.1016/j.diamond.2024.111524>
32. Mohammed LA, Majeed AH, Hammoodi OG, Prakash C, Alheety MA, Buddhi D, Dadoosh SA, Mohammed IK (2023) Design and characterization of novel ternary nanocomposite (rGO-MnO₂-PoPDA) product and screening its dielectric properties. *Int J Interact Des Manuf* 17:2387–2401. <https://doi.org/10.1007/s12008-022-01020-x>
33. Aksoy C, Anakli D (2019) Synthesis of Graphene Oxide Through Ultrasonic Assisted Electrochemical Exfoliation. *Open Chemistry* 17:581–586. <https://doi.org/10.1515/chem-2019-0062>
34. Anaklı D, Çetinkaya S (2010) Preparation of poly(2-ethyl aniline)/kaolinite composite materials and investigation of their properties. *Curr Appl Phys* 10:401–406. <https://doi.org/10.1016/j.cap.2009.06.037>
35. Anaklı D (2024) Influence of graphene concentration on the properties of the composite prepared with poly(2-ethyl aniline) by mechanochemical method. *Int J Mater Res* 115:208–220. <https://doi.org/10.1515/ijmr-2023-0098>
36. Blinova NV, Stejskal J, Trchová M, Prokeš J, Omastová M (2007) Polyaniline and polypyrrole: A comparative study of the preparation. *Eur Polym J* 43:2331–2341. <https://doi.org/10.1016/j.eurpolymj.2007.03.045>
37. Lamichhane P, Dhakal D, Jayalath IN, Baxter L, Chaudhari S, Vaidyanathan R (2022) Polyaniline and graphene nanocomposites for enhancing the interlaminar fracture toughness and thermomechanical properties of carbon fiber/epoxy composites. *arXiv preprint arXiv:2207.09500*. <https://doi.org/10.48550/arXiv.2207.09500>

38. Hidayah NMS, Liu WW, Lai CW, Noriman NZ, Khe CS, Hashim U, Lee HC (2017) Comparison on graphite, graphene oxide and reduced graphene oxide: Synthesis and characterization. AIP Conference Proceedings 1892. <https://doi.org/10.1063/1.5005764>
39. Sudesh Kumar N, Das S, Bernhard C, Varma GD (2013) Effect of graphene oxide doping on superconducting properties of bulk MgB₂. Supercond Sci Technol 26(9). <https://doi.org/10.1088/0953-2048/26/9/095008>
40. Rajagopalan B, Hur SH, Chung JS (2015) Surfactant-treated graphene covered polyaniline nanowires for supercapacitor electrode. Nanoscale Res Lett 10:183. <https://doi.org/10.1186/s11671-015-0888-1>
41. Mahla DK, Rahaman M, Khastgir D (2015) Composition-dependent electrical and dielectric properties of Polyaniline/Graphene composites produced by in situ polymerization technique. Polym Compos 36:445–453. <https://doi.org/10.1002/pc.22959>
42. Jaafar E, Kashif M, Sahari SK, Ngaini Z (2018) Study on morphological, optical and electrical properties of graphene oxide (GO) and reduced graphene oxide (rGO). Materials Science Forum 917:112-116. <https://doi.org/10.4028/www.scientific.net/msf.917.112>